

Supplementary Information for

Highly Stable Polysulfone Anion Exchange Membranes Incorporated with Bulky Alkyl Substituted Guanidinium Cation

Boxin Xue,^{a, b} Fen Wang,^{a, b} Jifu Zheng,^{a, b*} Shenghai Li,^{a, b}

and Suobo Zhang^{a, b, c*}

^a Key Laboratory of Polymer Ecomaterials, Changchun Institute of Applied Chemistry,
Chinese Academy of Sciences, 5625 Renmin Street, Changchun 130022, China

^b University of Science and Technology of China, Hefei 230026, China

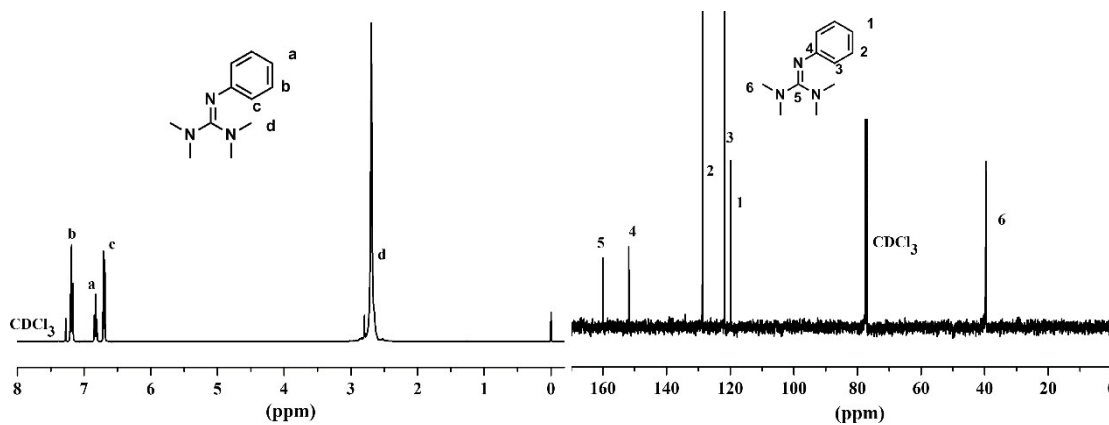
^c Jiangsu National Synergetic Innovation Center for Advanced Materials (SICAM), Nanjing
211816, China

* Corresponding author. E-mail: jfzheng@ciac.ac.cn; sbzhang@ciac.ac.cn.

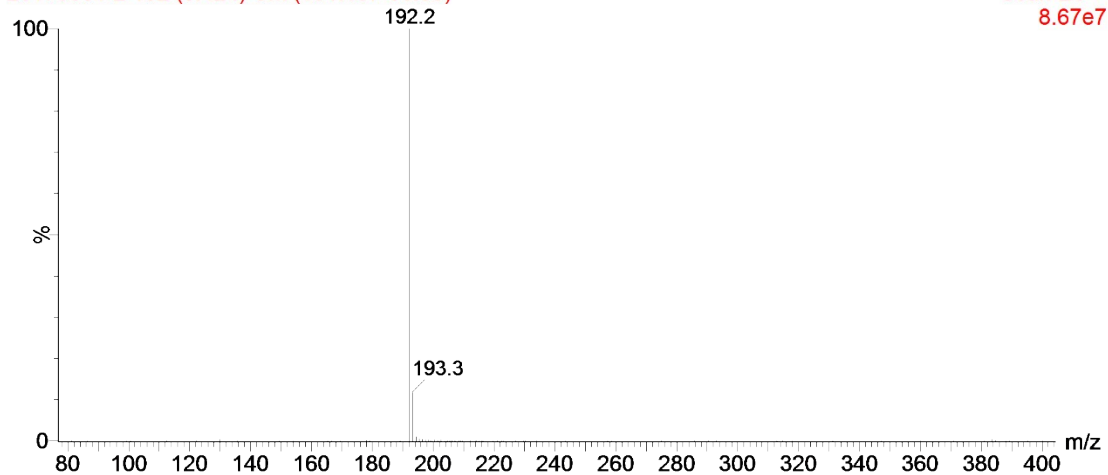
Contents

1. The ^1H NMR spectra, ^{13}C NMR spectra and mass spectra of guanidines and guanidinium model compounds.
2. The degradation of guanidinium model compounds M1–M3, M6 and M7–M9.
3. Figure S1. LUMO energy and isosurface of M3, M5 and M8.
4. Characterization of guanidinium functionalized aryl iodines, PSU-Bpin and AEMs.
 - 4.1. The ^1H NMR spectra, ^{13}C NMR spectra and mass spectra of guanidinium functionalized aryl iodines.
 - 4.2. Figure S2. The ^1H NMR spectra of PSU-Bpin, PSU-P-EG and PSU-P-PG.
 - 4.3. Figure S3. IR spectra of PSU-Bpin, PSU-P-EG and PSU-P-PG.
 - 4.4. Figure S4. AFM phase images of (A) PSU-P-EG and (B) PSU-P-PG. Scan box dimensions are $500\text{ nm} \times 500\text{ nm}$.
 - 4.5. Figure S5. The TGA curves of PSU-P-EG and PSU-P-PG.
 - 4.6. Table S1. Mechanical properties of PSU-P-EG and PSU-P-PG.
 - 4.7. Figure S6. (A) Water uptake and (B) swelling ratio of PSU-P-EG and PSU-P-PG.
 - 4.8. Figure S7. OH^- conductivity of PSU-P-EG and PSU-P-PG.

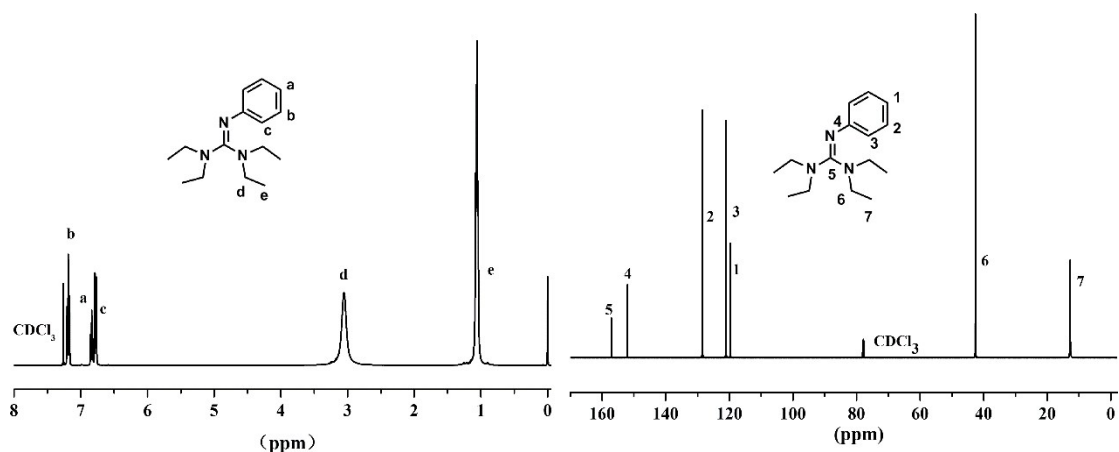
1,1,3,3-tetramethyl-2-phenylguanidine(G1) yield: 97.2%. ^1H NMR (400 MHz, CDCl_3): δ (ppm) 7.19 (2H, t), 6.83 (1H, t), 6.69 (2H, d), 2.69 (12H, s); ^{13}C NMR (100MHz, CDCl_3 ; ppm): δ 159.40, 151.48, 128.31, 121.53, 119.56, 39.63 ; HRMS (ESI): 192.2 $[\text{M}+\text{H}]^+$.



20170531-2 132 (3.424) Cm (131:137-56:59)

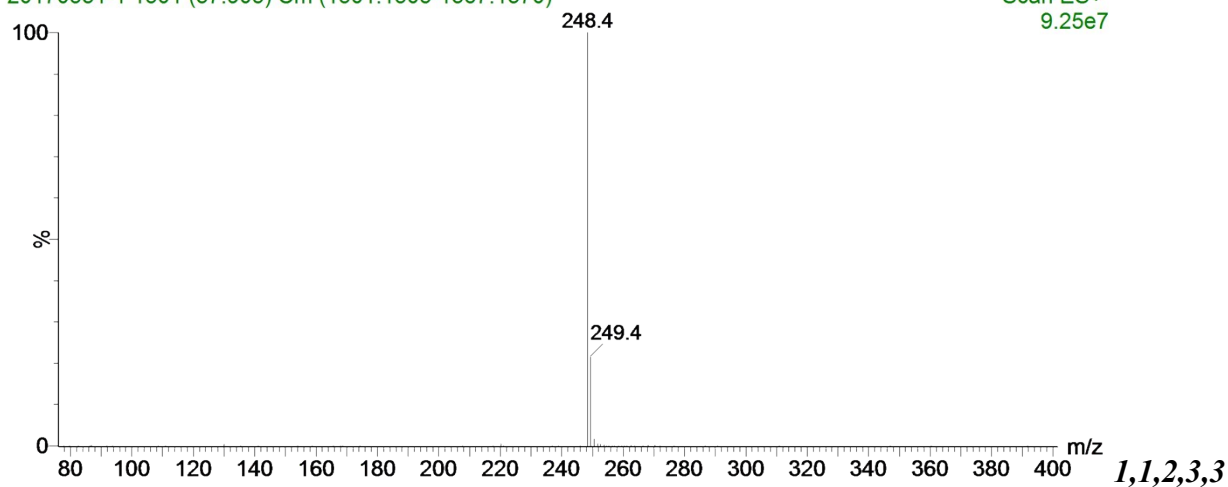


1,1,3,3-tetraethyl-2-phenylguanidine(G2) yield: 94.0%. ^1H NMR (400 MHz, CDCl_3): δ (ppm) 7.19 (2H, t), 6.83 (1H, t), 6.77 (2H, d), 3.05 (8H, s), 1.04(12H, t); ^{13}C NMR (100MHz, CDCl_3 ; ppm): δ 156.61, 151.83, 128.31, 121.08, 119.56, 42.11, 12.8; HRMS (ESI): 248.4 $[\text{M}+\text{H}]^+$.

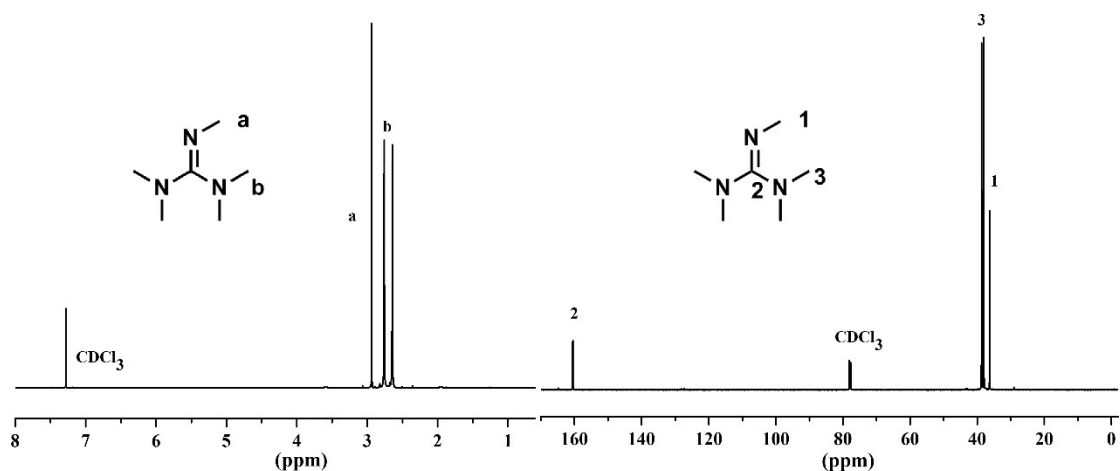


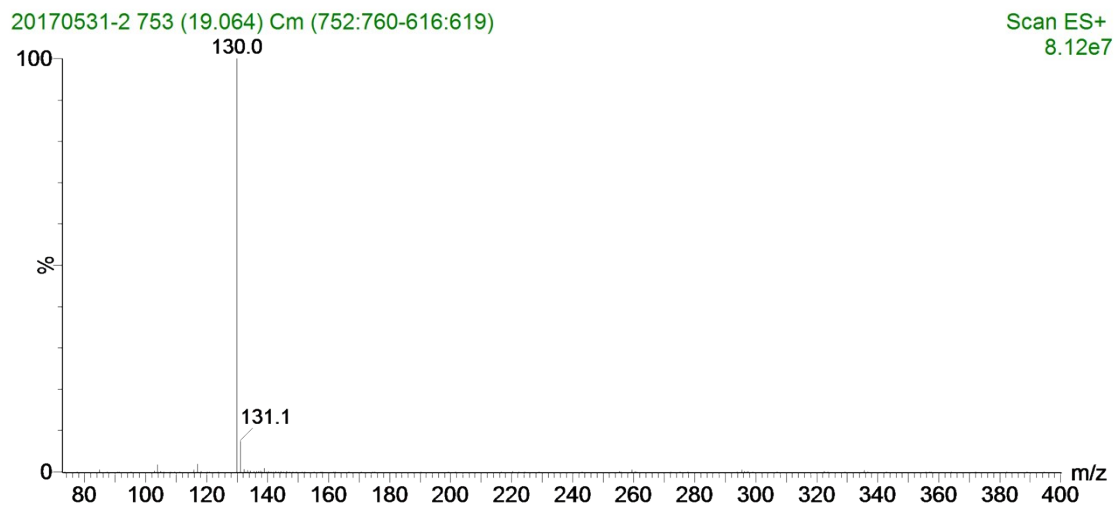
20170531-1 1501 (37.905) Cm (1501:1505-1367:1370)

Scan ES+
9.25e7

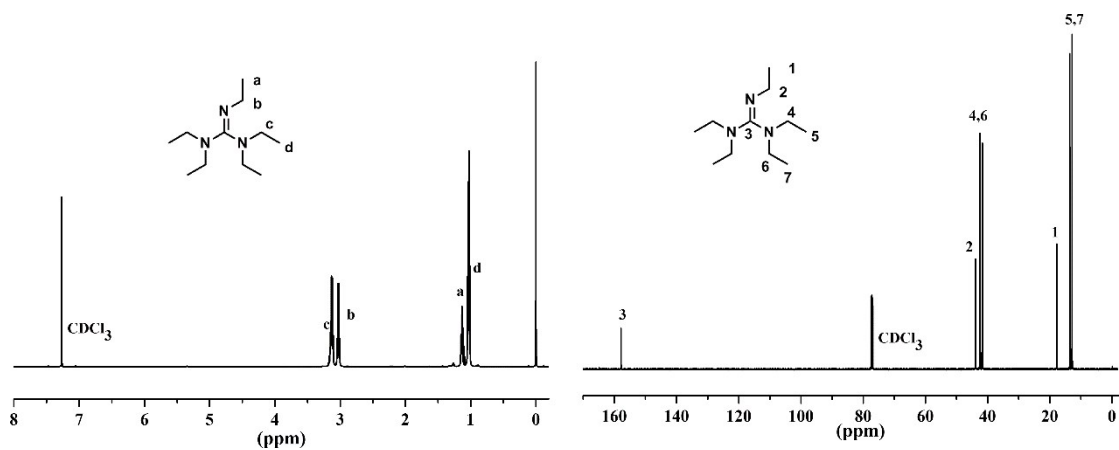


-pentamethylguanidine(G3) yield: 90.0%. ¹H NMR (400 MHz, CDCl₃): δ (ppm) 2.92 (3H, s), 2.74 (6H, s), 2.64 (6H, s); ¹³C NMR (100MHz, CDCl₃; ppm): δ 160.49, 38.06, 35.73; HRMS (ESI): 130.0 [M+H]⁺.



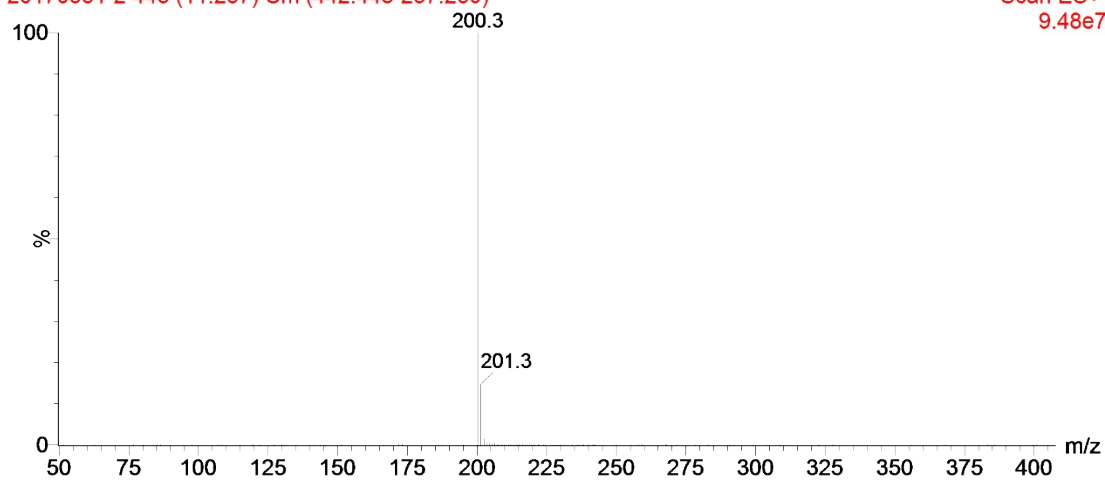


1,1,2,3,3-pentaethylguanidine(G4) yield: 97.5%. ^1H NMR (400 MHz, CDCl_3): δ (ppm) 3.01(2H, t), 3.11 (8H, mq), 1.01(8H, m), 1.13 (2H, d); ^{13}C NMR (100MHz, CDCl_3 ; ppm): δ 157.78, 43.76, 42.13, 41.32, 17.42, 13.46, 11.84 ; HRMS (ESI): 200.3 $[\text{M}+\text{H}]^+$.

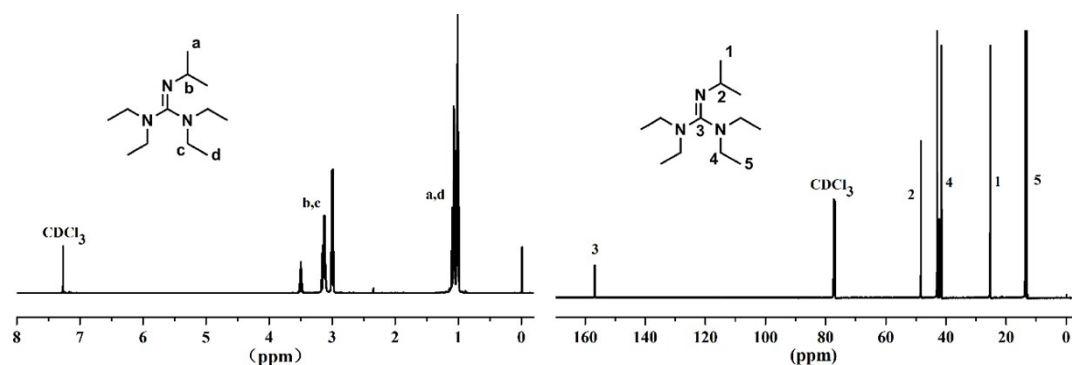


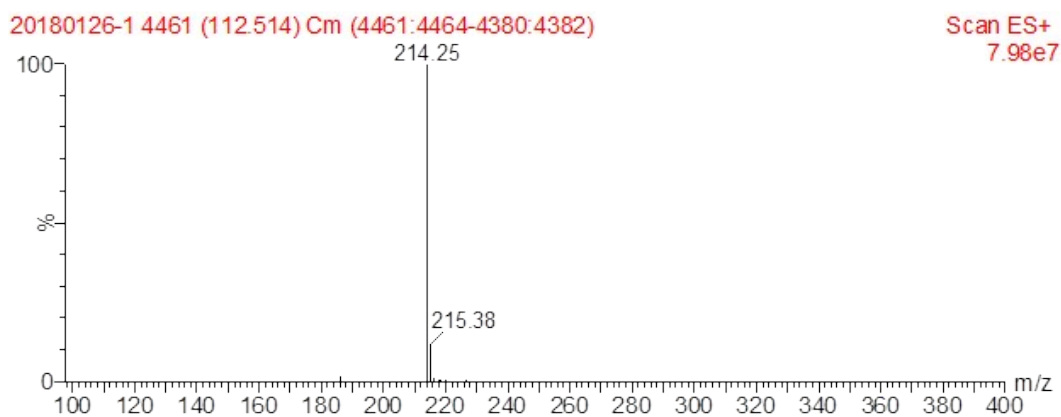
20170531-2 443 (11.257) Cm (442:448-257:260)

Scan ES+
9.48e7

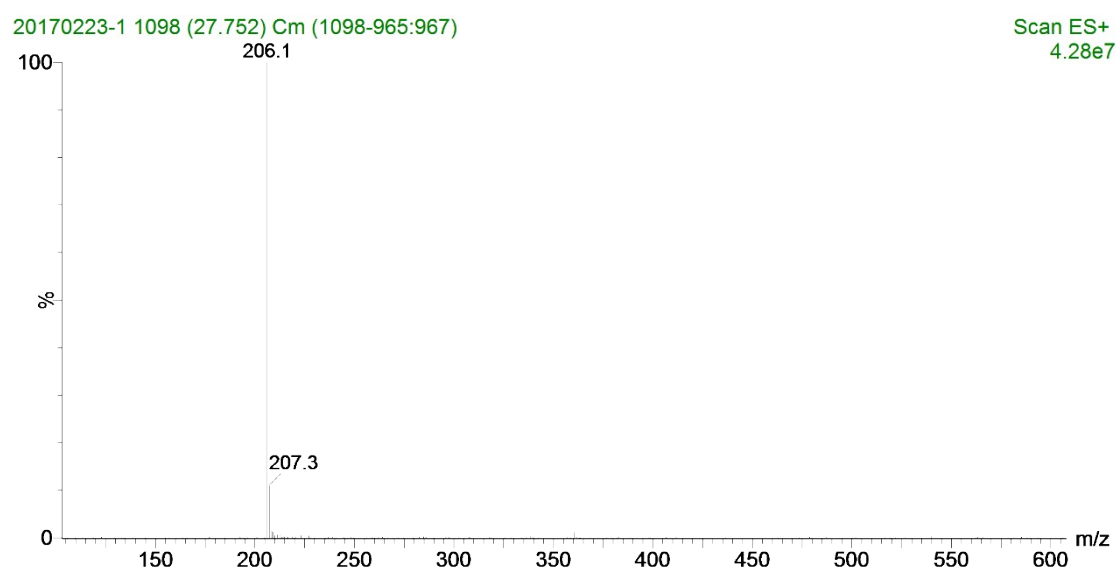
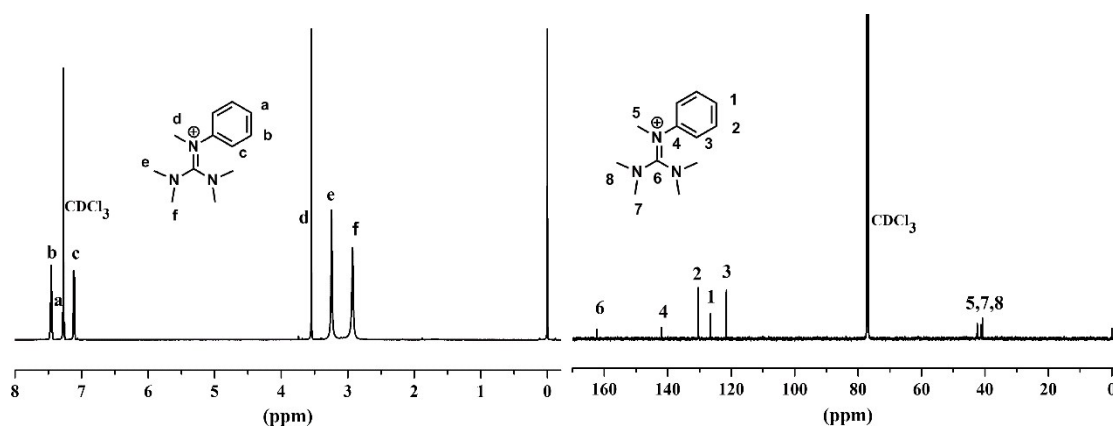


1,1,3,3-tetraethyl-2-isopropylguanidine (G5) yield: 93.0%. ^1H NMR (400 MHz, CDCl_3): δ (ppm) 3.49 (1H, m), 2.98-3.11 (8H, m), 1.02(18H, m); ^{13}C NMR (100MHz, CDCl_3 ; ppm): δ 156.91, 48.03, 43.07, 25.41, 13.62; HRMS (ESI): 214.25 $[\text{M}+\text{H}]^+$.

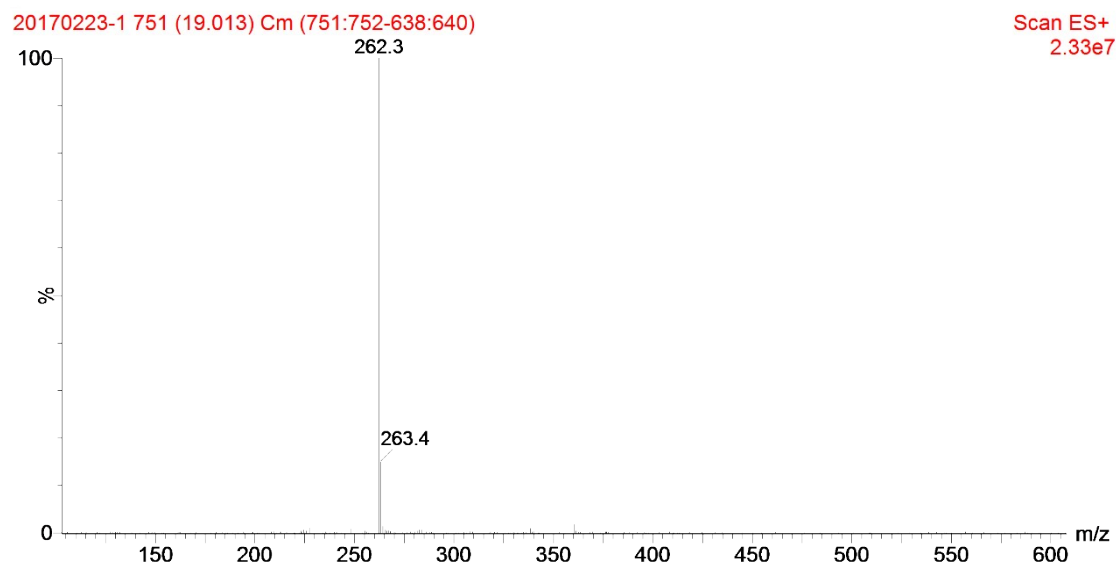
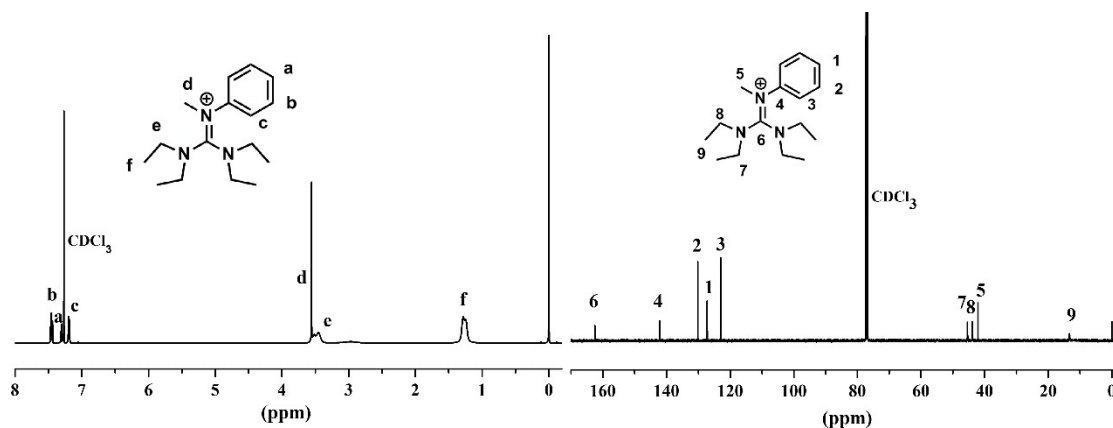




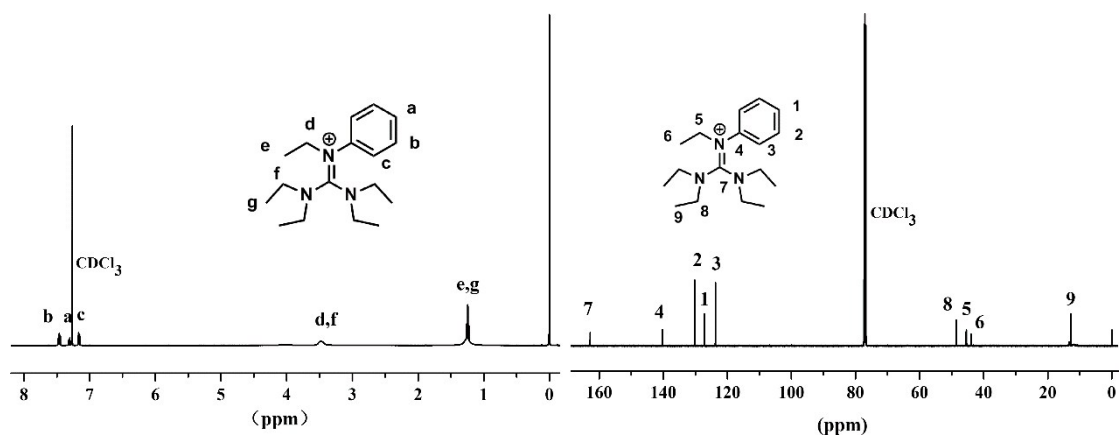
N-(bis(dimethylamino)methylene)-*N*-methylbenzenaminium iodide(M1), yield: 99.5%. ^1H NMR (400 MHz, CDCl_3): δ (ppm) 7.46 (2H, t), 7.27 (1H, t), 7.11 (2H, d), 3.55 (3H, s), 3.24(6H, s), 2.93(6H, s); ^{13}C NMR (100MHz, CDCl_3): δ (ppm) 162.33, 142.04, 130.38, 126.52, 121.52, 42.44, 41.23, 40.81; HRMS (ESI): 206.1 $[\text{M}]^+$.



***N*-(bis(diethylamino)methylene)-*N*-methylbenzenaminium iodide (M2)**, yield: 98.7%. ¹H NMR (400 MHz, CDCl₃): δ (ppm) 7.45 (2H, t), 7.30 (1H, t), 7.18 (2H, d), 3.56 (3H, s), 3.45(8H, s), 1.28(12H, m); ¹³C NMR (100MHz, CDCl₃): δ (ppm) 162.54, 142.15, 130.18, 127.20, 123.00, 45.40, 43.83, 42.09, 13.32; HRMS (ESI): 262.3 [M]⁺.

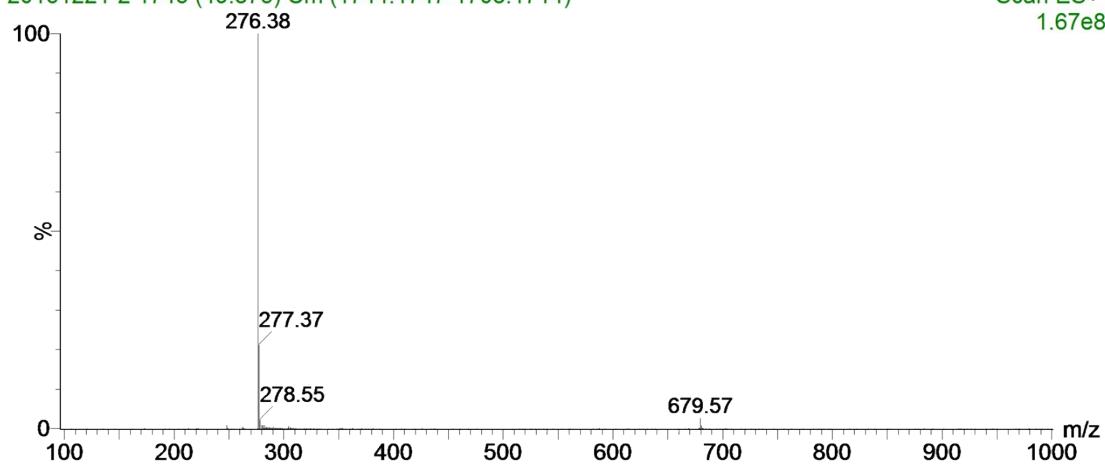


***N*-(bis(diethylamino)methylene)-*N*-ethylbenzenaminium iodide (M3)**, yield: 99.0%. ¹H NMR (400 MHz, CDCl₃): δ (ppm) 7.46 (2H, t), 7.30 (1H, t), 7.17 (2H, d), 3.48 (10H, s), 1.24(15H, t); ¹³C NMR (100MHz, CDCl₃; ppm): δ 162.83, 140.30, 130.16, 127.15, 123.72, 48.56, 45.42, 43.93, 13.26; HRMS (ESI): 276.38 [M]⁺.



20161221-2 1745 (49.875) Cm (1744:1747-1708:1714)

Scan ES+
1.67e8

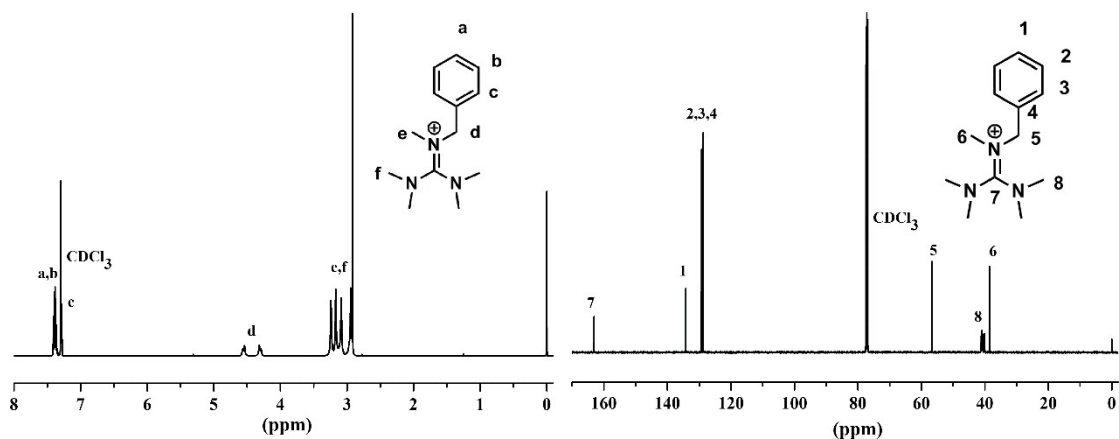


N-(bis(dimethylamino)methylene)-*N*-methyl-1-phenylmethanaminium chloride (M4), yield:

95.5%. ¹H NMR (400 MHz, CDCl₃): δ (ppm) 7.20-7.40 (5H, m), 4.30 (2H, q), 4.45 (2H, q),

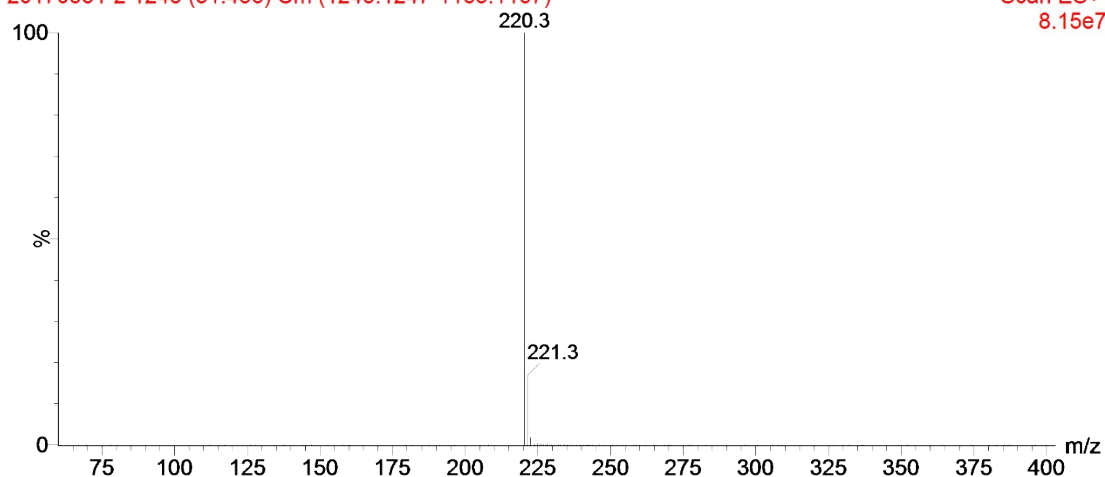
2.93-3.18 (15H, m); ¹³C NMR (100MHz, CDCl₃; ppm): δ 163.01, 134.21, 129.10, 127.92,

56.54, 40.13, 38.55 ; HRMS (ESI): 220.3 [M]⁺.

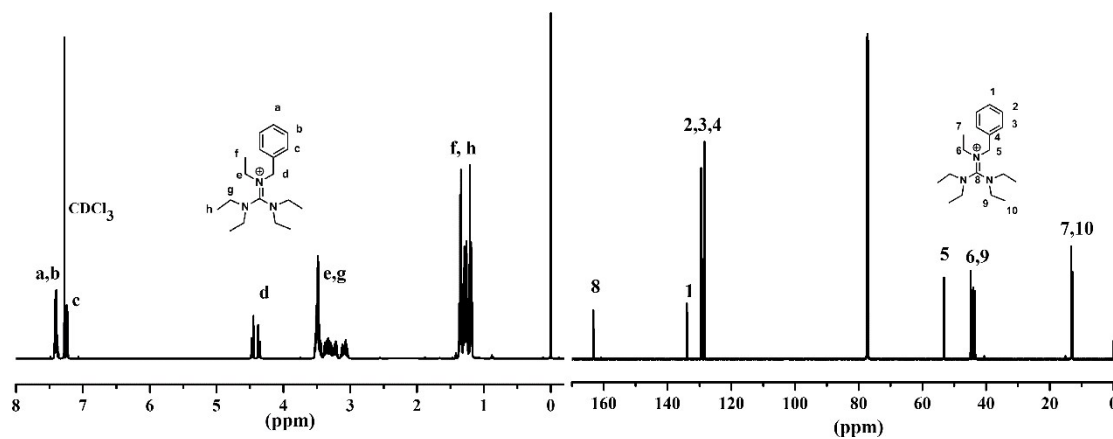


20170531-2 1245 (31.456) Cm (1245:1247-1165:1167)

Scan ES+
8.15e7

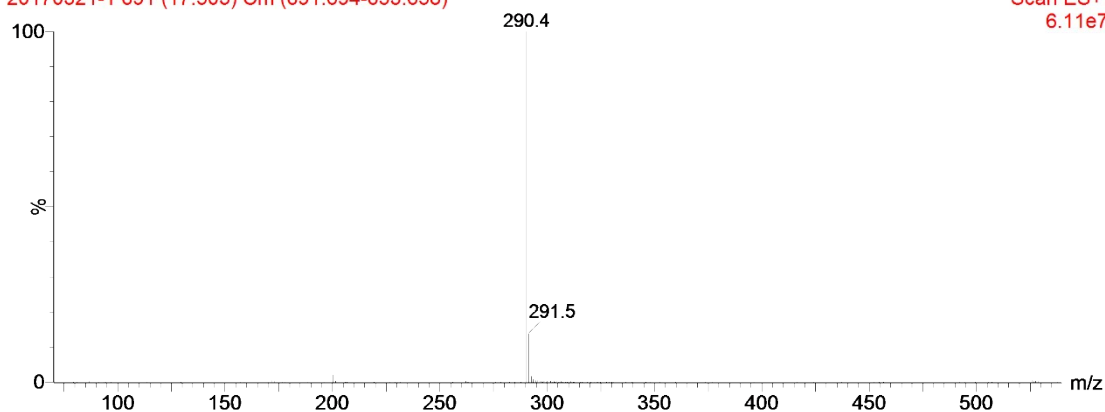


N-benzyl-*N*-(bis(diethylamino)methylene)ethaniminium chloride (**M5**), yield: 98.5%. ^1H NMR (400 MHz, CDCl_3): δ (ppm) 7.39 (3H, m), 7.23 (2H, d), 4.45 (2H, q), 3.00-3.55 (10H, m), 1.15-1.40 (15H, m); ^{13}C NMR (100MHz, CDCl_3 ; ppm): δ 163.23, 133.89, 129.46, 129.15, 128.40, 53.27, 44.91, 44.03, 13.24, 13.12 ; HRMS (ESI): 290.4 $[\text{M}]^+$.



20170321-1 691 (17.503) Cm (691:694-653:658)

Scan ES+
6.11e7



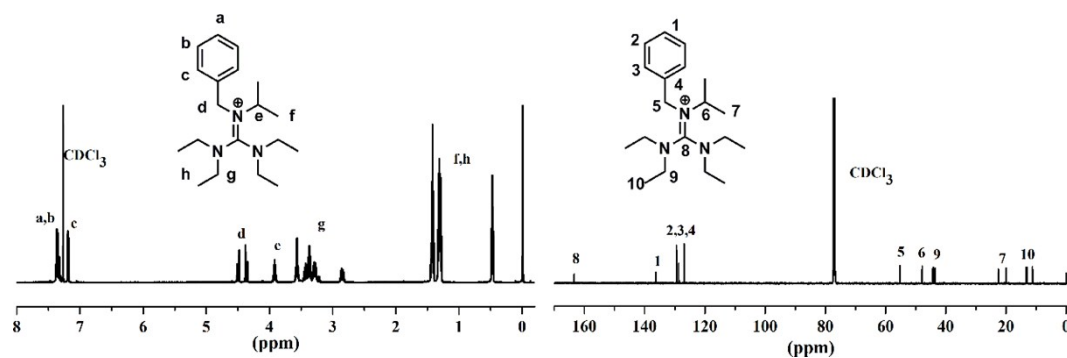
N-benzyl-*N*-(bis(diethylamino)methylene)propan-2-aminium chloride (**M6**), yield: 80.5%.

^1H NMR (400 MHz, CDCl_3): δ (ppm) 7.37 (3H, m), 7.19 (2H, d), 4.48 (2H, q), 3.92 (1H, m),

2.85-3.57 (8H, m), 0.45-1.41 (18H, m); ^{13}C NMR (100MHz, CDCl_3 ; ppm): δ 163.40, 135.91,

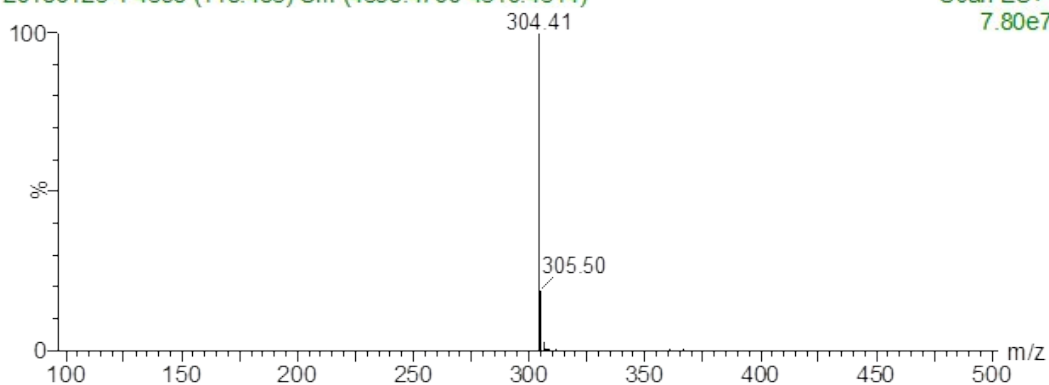
129.42, 128.79, 126.90, 55.33, 48.03, 44.03, 43.61, 22.06, 20.45, 12.88, 10.71 ; HRMS (ESI):

304.41 $[\text{M}]^+$.

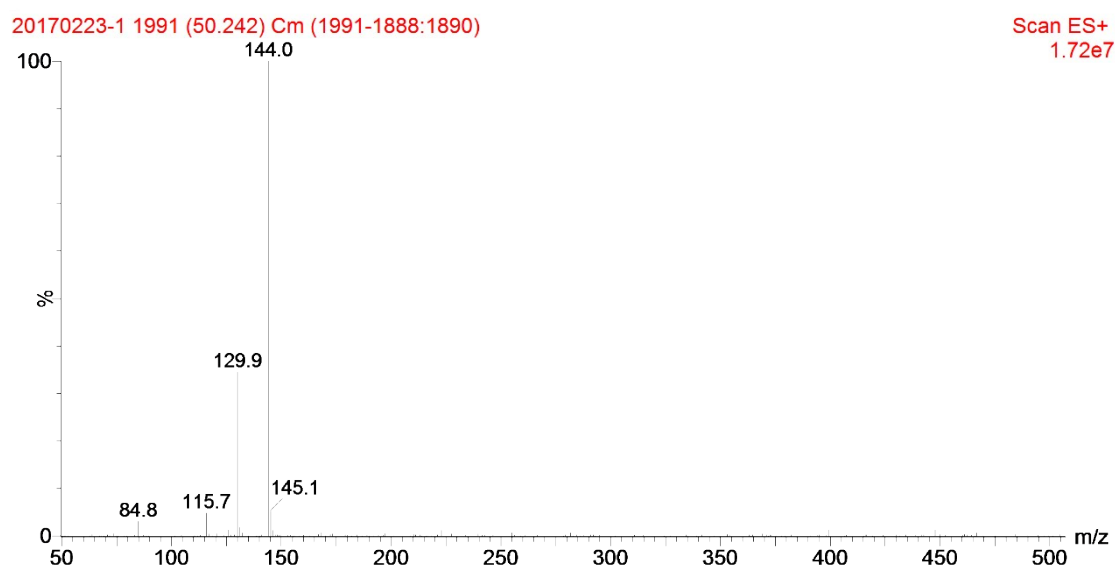
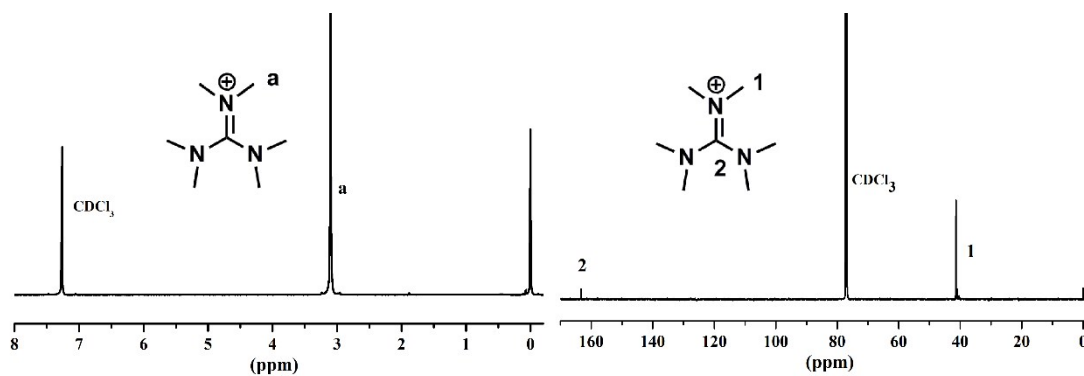


20180126-1 4698 (118.486) Cm (4698:4700-4610:4614)

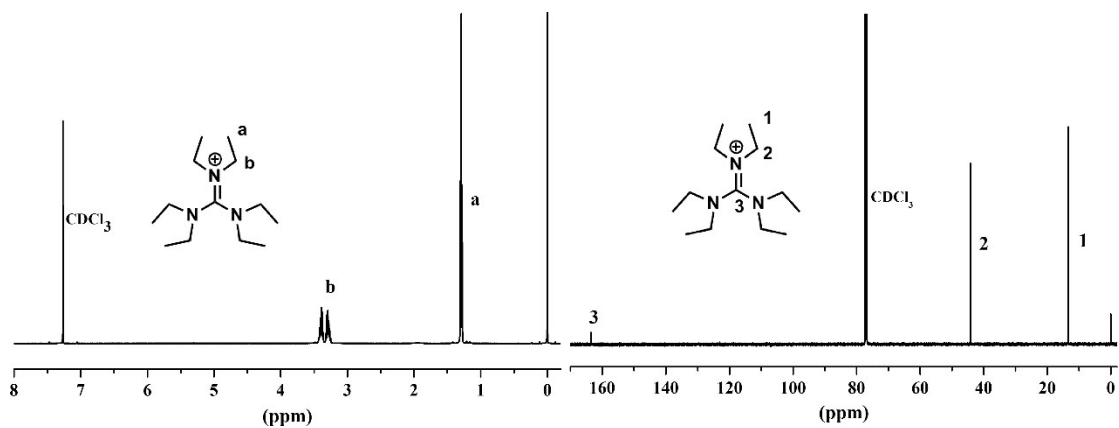
Scan ES+
7.80e7



N-(bis(dimethylamino)methylene)-*N*-methylethanaminium iodide(M7), yield: 99.2%. ^1H NMR (400 MHz, CDCl_3): δ (ppm) 3.10 (12H, s); ^{13}C NMR (100MHz, CDCl_3): δ (ppm) 163.36, 41.41; HRMS (ESI): 144.0 $[\text{M}]^+$.

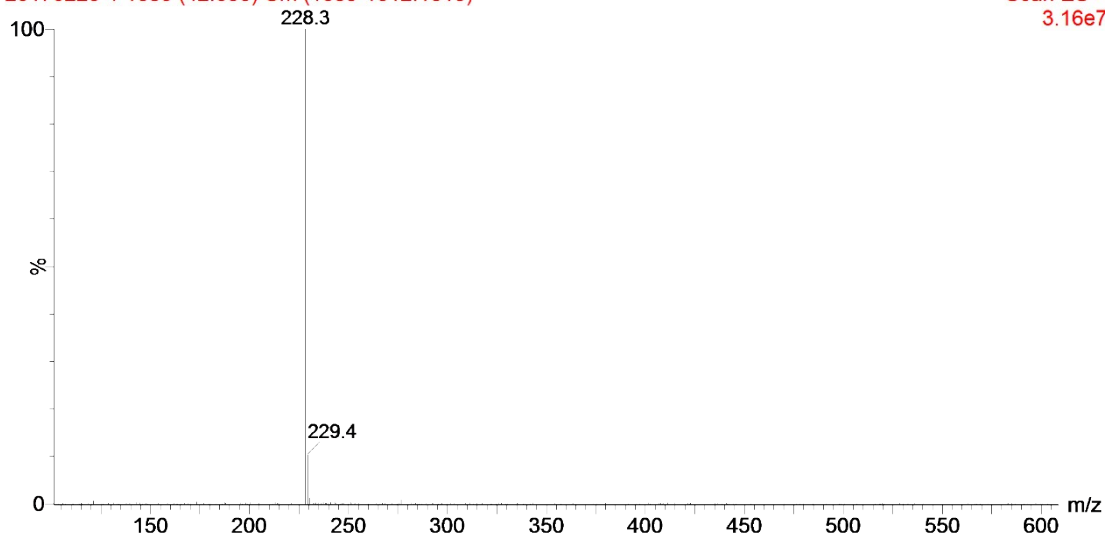


N-(bis(diethylamino)methylene)-*N*-ethylethanaminium iodide(M8), yield: 97.8%. ^1H NMR (400 MHz, CDCl_3): δ (ppm) 3.38 (12H, m), 1.29 (18H, t); ^{13}C NMR (100MHz, CDCl_3): δ (ppm) 163.54, 44.21, 13.39; HRMS (ESI): 228.3 $[\text{M}]^+$.

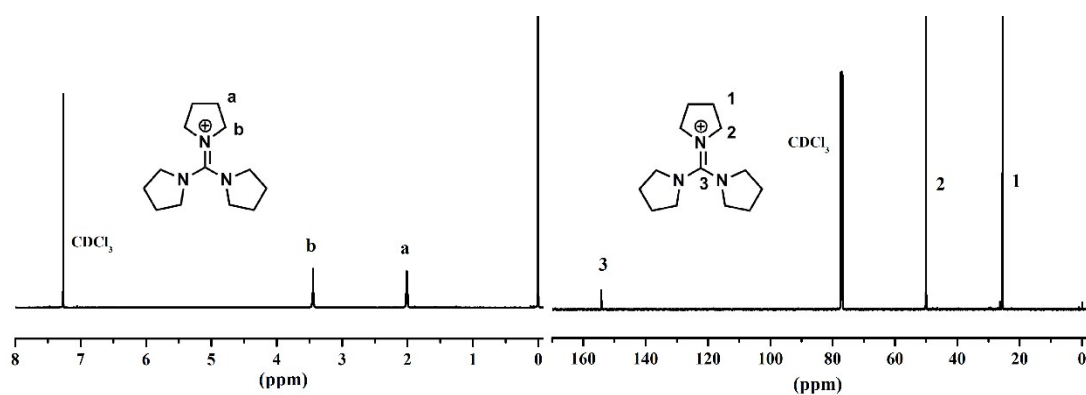


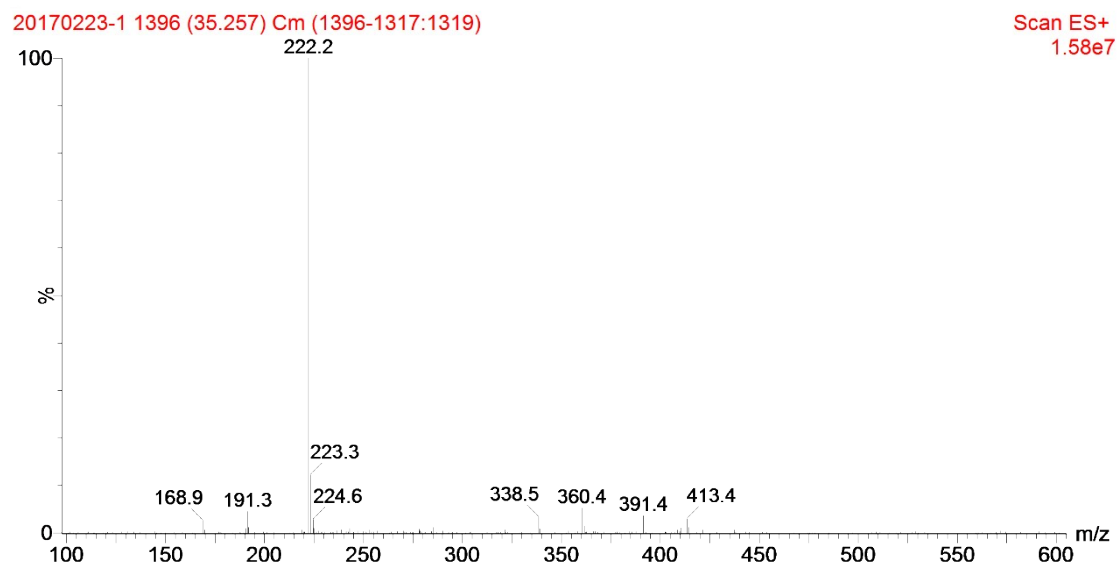
20170223-1 1689 (42.636) Cm (1689-1612:1613)

Scan ES+
3.16e7

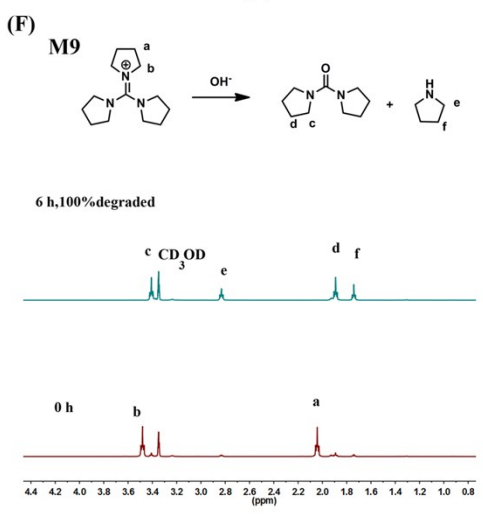
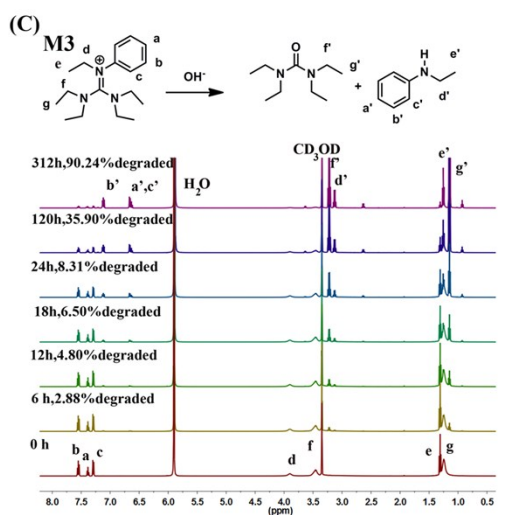
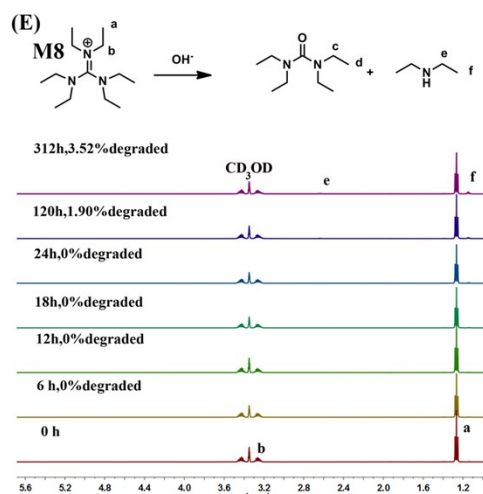
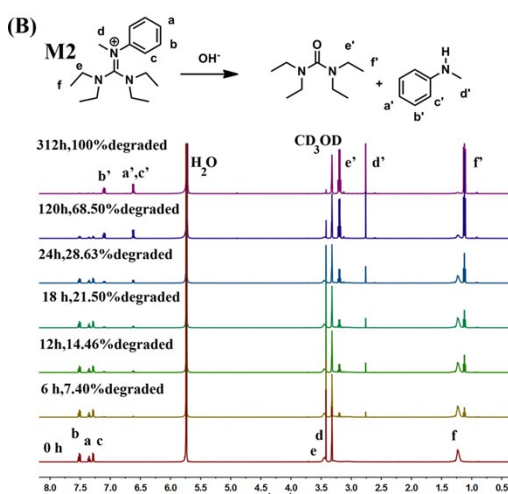
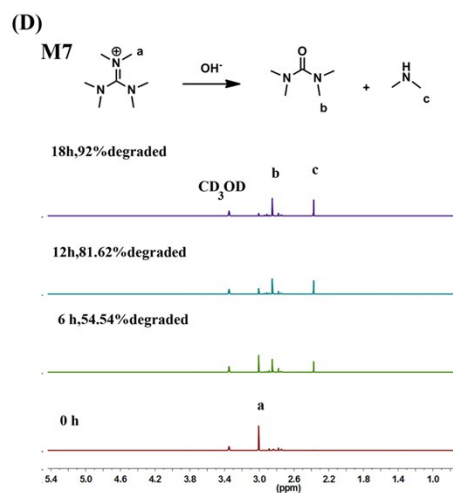
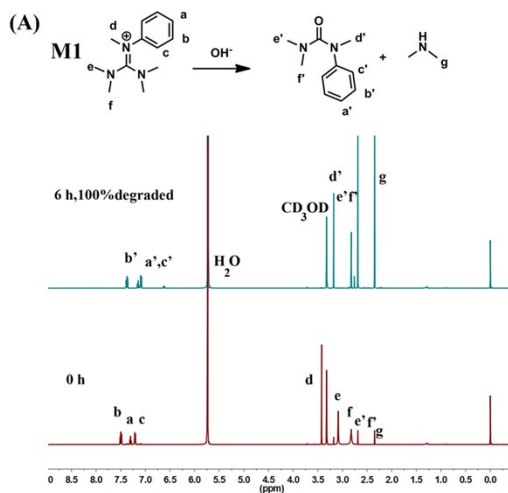


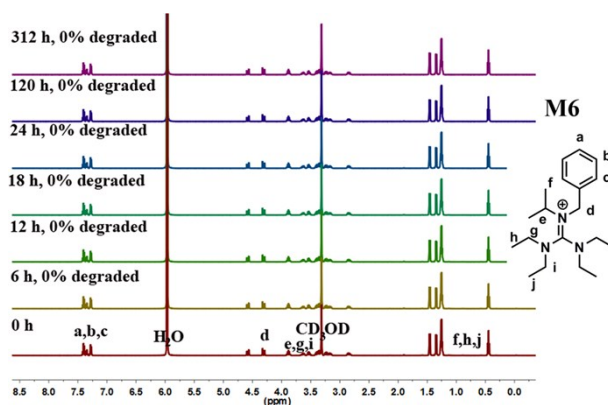
1-(di(pyrrolidin-1-yl)methylene)pyrrolidin-1-ium chloride(M9), yield: 99.0%. ^1H NMR (400 MHz, CDCl_3): δ (ppm) 3.56 (8H, m), 2.02 (8H, m); ^{13}C NMR (100MHz, CDCl_3): δ (ppm) 154.18, 26.32; HRMS (ESI): 222.2 $[\text{M}]^+$.





The degradation of guanidinium model compounds M1–M3, M6 and M7–M9:





Theoretical calculations were carried out using Gaussian03 and Gaussian09 program packages.^{1,2} The geometric optimization of both the structures and transition states were initially carried out at the B3LYP/6-31+G(d) level. The connection of each transition state to associated structures or fragments was checked by the intrinsic reaction coordinate (IRC) method at the B3LYP/6-31+G(d) level. To get detailed orbital information, we performed the natural bond orbital (NBO) analysis.

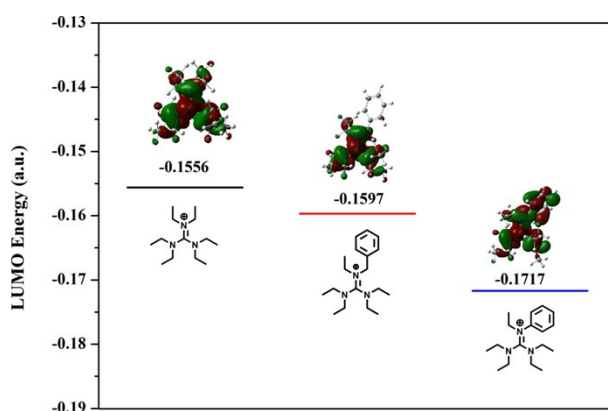
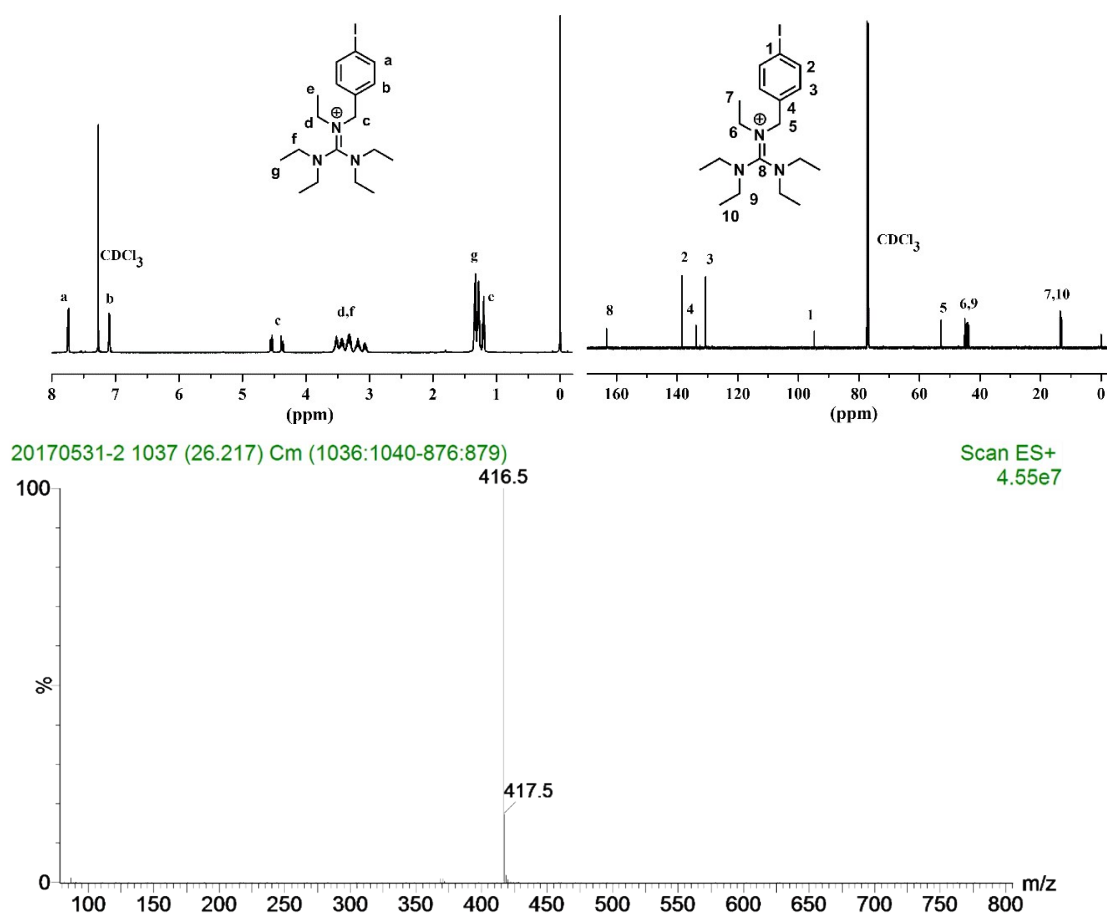


Figure S1. LUMO energy and isosurface of M3, M5 and M8.

Guanidiniums functionalized aryl iodines: *N*-(bis(diethylamino)methylene)-*N*-(4-iodobenzyl)ethanaminium (GI-E). ¹H NMR (400 MHz, CDCl₃): δ (ppm) 7.74 (2H, d), 7.08 (2H, d), 4.52 (2H, q), 3.07-3.52 (10H, m), 1.19-1.35(15H, m); ¹³C NMR (100MHz, CDCl₃; ppm): δ 163.32, 138.26, 133.48, 130.24, 94.37, 52.44, 44.51, 43.34, 13.42, 12.61; HRMS

(ESI): 416.5 [M]⁺.



Guanidiniums functionalized aryl iodines: *N*-(bis(diethylamino)methylene)-*N*-(4-iodobenzyl)propan-2-aminium (GI-P). ¹H NMR (400 MHz, CDCl₃): δ (ppm) 7.65(2H, d), 7.01 (2H, d), 4.42 (2H, q), 2.84-3.84 (9H, m), 0.56-1.36(18H, m); ¹³C NMR (100MHz, CDCl₃; ppm): δ 163.13, 138.61, 135.91, 129.15, 93.19, 55.60, 47.13, 43.88, 22.43, 20.18, 13.42, 11.80; HRMS (ESI): 430.4[M]⁺.

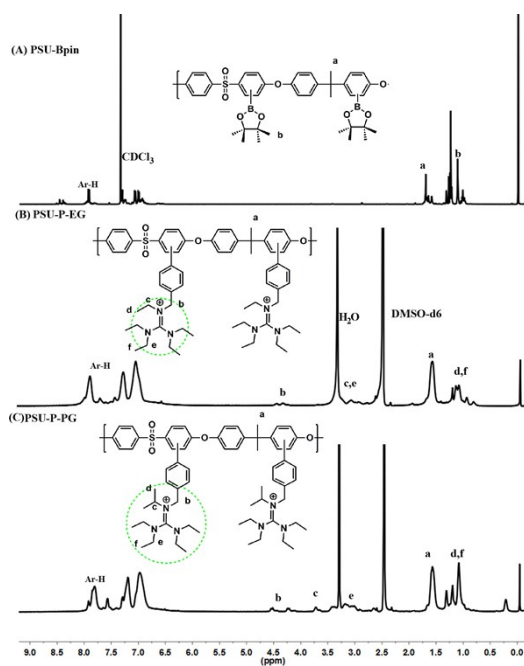


Figure S2. The ^1H NMR spectra of PSU-Bpin, PSU-P-EG and PSU-P-PG.

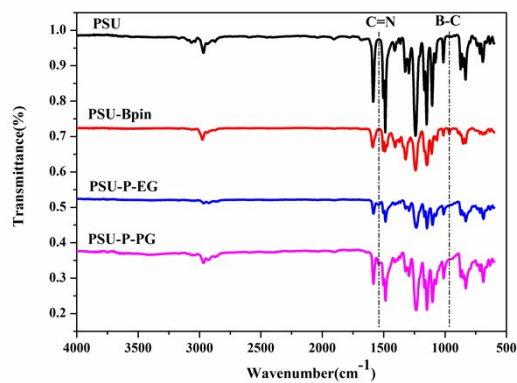


Figure S3. IR spectras of PSU-Bpin, PSU-P-EG and PSU-P-PG.

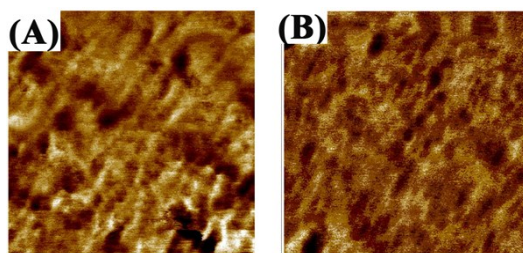


Figure S4. AFM phase images of (A) PSU-P-EG and (B) PSU-P-PG. Scan box dimensions are $500\text{ nm} \times 500\text{ nm}$.

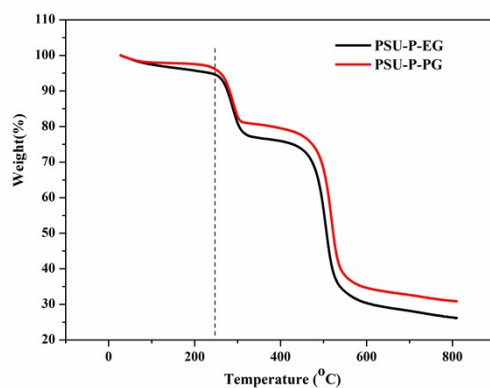


Figure S5. The TGA curves of PSU-P-EG and PSU-P-PG.

Table S1. Mechanical properties of PSU-P-EG and PSU-P-PG.

sample	TS ^a (MPa)	YM ^a (MPa)	EB ^a (%)
PSU-P-EG	52.1	1489	9.9
PSU-P-PG	40.0	1160	5.7

^a TS: Tensile strength; YM: Young's modulus; EB: Elongation at break.

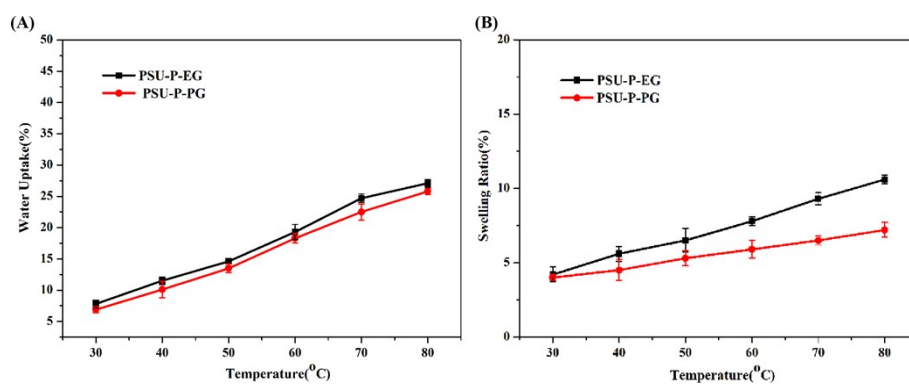


Figure S6. (A) Water uptake and (B) swelling ratio of PSU-P-EG and PSU-P-PG.

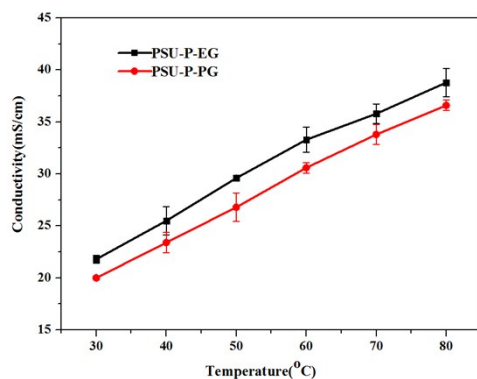


Figure S7. OH^- conductivity of PSU-P-EG and PSU-P-PG.

References

1. M. J. Frisch, G. W. Trucks, H. B. Schlegel, G. E. Scuseria, M. A. Robb, J. R. Cheeseman, J. A. Montgomery Jr T. Vreven, K. N. Kudin, J. C. Burant, J. M. Millam, S. S. Iyengar, J. Tomasi, V. Barone, B. Mennucci, M. Cossi, G. Scalmani, N. Rega, G. A. Petersson, H. Nakatsuji, M. Hada, M. Ehara, K. Toyota, R. Fukuda, J. Hasegawa, M. Ishida, T. Nakajima, Y. Honda, O. Kita, H. Nakai, M. Klene, X. Li, J. E. Knox, H. P. Hratchian, J. B. Cro, V. Bakken, C. Adamo, J. Jaramillo, R. Gomperts, R. E. Stratmann, O. Yazyev, A. J. Austin, R. Cammi, C. Pomelli, J. W. Ochterski, P. Y. Ayala, K. Morokuma, G. A. Voth, P. Salvador, J. J. Dannenbe, V. G. Zakrzewski, S. Dapprich, A. D. Daniels, M. C. Strain, O. Farkas, D. K. Malick, A. D. Rabuck, K. Raghavachari, J. B. Foresman, J. V. Ortiz, Q. Cui, A. G. Baboul, S. Clifford, J. Cioslowski, B. B. Stefanov, G. Liu, A. Liashenko, P. Piskorz, I. Komaromi, R. L. Martin, D. J. Fox, T. Keith, M. A. AlLaham, C. Y. Peng, A. Nanayakkara, M. Challacombe, P. M. W. Gill, B. Johnson, W. Chen, M. W. Wong, C. Gonzalez and J. A. Pople, Gaussian 09, Revision D.01, Gaussian, Inc., Wallingford, CT, 2004.
2. M. J. Frisch, G. W. Trucks, H. B. Schlegel, G. E. Scuseria, M. A. Robb, J. R. Cheeseman, G. Scalmani, V. Barone, B. Mennucci, G. A. Petersson, H. Nakatsuji, M. Caricato, X. Li, H. P. Hratchian, A. F. Izmaylov, J. Bloino, G. Zheng, J. L. Sonnenberg, M. Hada, M.

Ehara, K. Toyota, R. Fukuda, J. Hasegawa, M. Ishida, T. Nakajima, Y. Honda, O. Kitao, H. Nakai, T. Vreven, J. A. Montgomery Jr, J. E. Peralta, F. Ogliaro, M. Bearpark, J. J. Heyd, E. Brothers, K. N. Kudin, V. N. Staroverov, R. Kobayashi, J. Normand, K. Raghavachari, A. Rendell, J. C. Burant, S. S. Iyengar, J. Tomasi, M. Cossi, N. Rega, J. M. Millam, M. Klene, J. E. Knox, J. B. Cross, V. Bakken, C. Adamo, J. Jaramillo, R. Gomperts, R. E. Stratmann, O. Yazyev, A. J. Austin, R. Cammi, C. Pomelli, J. W. Ochterski, R. L. Martin, K. Morokuma, V. G. Zakrzewski, G. A. Voth, P. Salvador, J. J. Dannenberg, S. Dapprich, A. D. Daniels, O. Farkas, J. B. Foresman, J. V. Ortiz, J. Cioslowski and D. J. Fox, Gaussian 03, Revision D.02, Gaussian, Inc., Wallingford, CT, 2009.